INTERNATIONAL JOURNAL FOR NUMERICAL METHODS IN ENGINEERING
Int. J. Numer. Meth. Engng 2003; **57**:103–116 (DOI: 10.1002/nme.673)

Non-local boundary integral formulation for softening damage

Ján Sládek[1], Vladimír Sládek[1] and Zdeněk P. Bažant[2,*,†]

[1] *Institute of Construction and Architecture, Slovak Academy of Sciences, 84220 Bratislava, Slovakia*
[2] *Department of Civil Engineering, Northwestern University, Evanston, Illinois 60208, U.S.A.*

SUMMARY

A strongly non-local boundary element method (BEM) for structures with strain-softening damage treated by an integral-type operator is developed. A plasticity model with yield limit degradation is implemented in a boundary element program using the initial-stress boundary element method with iterations in each load increment. Regularized integral representations and boundary integral equations are used to avoid the difficulties associated with numerical computation of singular integrals. A numerical example is solved to verify the physical correctness and efficiency of the proposed formulation. The example consists of a softening strip perforated by a circular hole, subjected to tension. The strain-softening damage is described by a plasticity model with a negative hardening parameter. The local formulation is shown to exhibit spurious sensitivity to cell mesh refinements, localization of softening damage into a band of single-cell width, and excessive dependence of energy dissipation on the cell size. By contrast, the results for the non-local theory are shown to be free of these physically incorrect features. Compared to the classical non-local finite element approach, an additional advantage is that the internal cells need to be introduced only within the small zone (or band) in which the strain-softening damage tends to localize within the structure. Copyright © 2003 John Wiley & Sons, Ltd.

KEY WORDS: non-local models; boundary elements; damage; fracture; softening; computational mechanics

1. INTRODUCTION

The continuum damage mechanics has been established to fill the gap between the classical continuum mechanics and fracture mechanics. Unless very large structures are considered, the classical linear elastic fracture mechanics cannot be directly applied to heterogenous quasi-brittle materials such as concrete, heterogeneous rocks, sea ice, fiber composites, and toughened ceramics, due to the existence of a sizable fracture process zone containing a large number of distributed microcracks at the fracture front. A continuum model for microcracking

*Correspondence to: Zdeněk Bažant, McCormick School Professor and W. P. Murphy Professor of Civil Engineering and Materials Science, Northwestern University, 2145 Sheridan Road, CEE Rm A135, Evanston, Illinois 60208, U.S.A.
†E-mail: z-bazant@northwestern.edu

Contract/grant sponsor: U.S. National Science Foundation, Northwestern University; contract/grant number: CMS-9713944

Received 7 August 2001
Revised 19 April 2002
Accepted 12 July 2002

in these materials leads inevitably to strain softening, which causes a loss of positive definiteness of the elastic moduli matrix and thus leads to an ill-posed boundary value problem [1, 2]. Finite element calculations using elasto-plastic models with yield limit degradation in the framework of the classical (local) theory of plasticity give very different results for different discretization meshes [3]. The results are not objective with respect to the finite element mesh refinements and converge at infinite mesh refinement to a solution with zero energy dissipation during failure.

To prevent such physically unrealistic behaviour, one must introduce mathematical models called localization limiters, which force the strain-softening region to have a certain minimum finite size [4–9]. A useful localization limiter is the non-local continuum concept, which was initially introduced in elasticity for an entirely different purpose [10, 11]. An effective non-local model, proposed in References [12, 13], is the non-local continuum with local strain, which treats as non-local only those variables that cause strain-softening, the other variables being considered as local. This type of non-local concept may be applied to all kinds of constitutive models with strain softening [9]. A recent critical review of various non-local models is given by Jirásek [14], and a comprehensive review by Bažant and Jirásek [15].

The boundary element method (BEM) has already become a popular alternative to the well-established finite element method (FEM). The main advantage of the BEM in comparison with the domain techniques consists in the reduction of the number of unknowns. It is a powerful tool in linear elasticity, but it has been found efficient also in inelastic material problems.

The earliest BEM formulations for elastoplasticity were due to Swedlow and Cruse [16]. The first two-dimensional analyses were given by Ricardella [17], and the first two-dimensional viscoplastic analyses were presented by Chaudonneret [18], and Kumar and Mukherjee [19]. Banerjee *et al.* [20] demonstrated the first applications of the method to three-dimensional elastoplastic problems while Banerjee and Cathie [21] presented the first axisymmetric elastoplastic analyses.

Since their beginnings, the inelastic formulations have been considerably improved [22–25]. The BEM solution algorithm uses incremental loading, for which an accurate computation of the stress rates is a crucial point, required to ensure good convergence of the results for inelastic material problems. Regularization or singularity removal before numerical computation can make the BEM an efficient and generally well-conditioned numerical solution procedure.

The regularization techniques for integral representation of stresses in elasticity [26] and for an extension to the stress rates in elastoplasticity [27] are applied in this paper. Beside the boundary integrals, also the domain integrals [28, 29] are to be regularized in proper formulations for BEM solution of elastoplastic problems. Then, the integration over the boundary and domain elements can be performed sufficiently accurately by using a standard quadrature for numerical integration.

An important development, due to Maier *et al.* [30–33], was the formulation of the symmetric Galerkin-type boundary element method, which endows all the key operators with symmetry. In a combined static-kinematic formulation, this method uses Galerkin weighted residual enforcement of integral equations for displacements and tractions along the boundary and for stresses in the plastic domain, and space discretization in terms of generalized variables. The method was shown effective for elastoplastic problems, including shakedown.

This method was further extended to a weakly non-local formulation of gradient plasticity [34, 35], in which the inelastic strain field in an infinitely close neighbourhood of a continuum point is taken into account through a Laplacian of the plastic hardening parameter. Owing to the presence of a characteristic material length in the gradient operator, this formulation admits negative values of this parameter, corresponding to material softening. Although no numerical demonstrations were included in Reference [34], this gradient formulation of Maier's group appears to be the first boundary element method that can in principle be applied to softening problems without resulting in a loss of ellipticity and ill-posedness of boundary value problem, spurious mesh sensitivity and lack of convergence.

The present study deals with a strongly non-local formulation in which a finite neighbourhood of a continuum point is taken into account through an integral operator. This integral-type non-local formulation for material softening, which is usually more effective than the weakly non-local formulation for treating problems with softening damage, for example distributed cracking, has apparently not yet been presented in the literature (except for the preceding study [36]) and is taken as the objective of this paper.

After formulating the theory, the numerical example of a perforated strip (a finite strip with a hole), subjected to tension, is analysed to verify the efficiency of the non-local formulation. Because of its simplicity, the von Mises plasticity model with a negative hardening parameter is used to describe the strain-softening damage in the material. Not surprisingly, the results for the local version of the theory exhibit after the peak of the stress–strain curve an instability, manifested by spurious oscillations. The non-local theory, by contrast, is shown to exhibit no spurious oscillations and to yield, for the damage zone with yield limit degradation, a load-deflection response that decreases monotonically.

In a parallel study [36], in which a simpler, but theoretically less appealing, version of the boundary element method is generalized for non-local behaviour, other numerical examples are analysed to confirm that the concept of a non-local plasticity model exhibits correct and rapid convergence at mesh refinements and avoids spurious mesh sensitivity. In that study, for the sake of simplicity, only the standard non-regularized integral representations are used. However, due to nearly singular kernels, such an integral representation does not allow accurate stress computation for points close to the boundary. For various numerical as well as physical reasons, this leads to spurious oscillations in the response curves for the local theory with a negative hardening modulus. To eliminate this source of numerical errors, the present formulation uses a regularized integral representation of stresses. The regularization or singularity removal before the numerical computation makes the BEM an efficient and generally well-conditioned numerical solution procedure.

2. BOUNDARY INTEGRAL FORMULATION FOR ELASTOPLASTICITY

We are interested in problems that can be solved under the assumption of small (linearized) strains, which represent a majority of practical situations. Then the governing elastoplastic stress–strain relation in terms of displacements may be written as [37]:

$$(\lambda_e + \mu)\dot{u}_{j,ji} + \mu\dot{u}_{i,jj} = \dot{\sigma}^{p}_{ij,j} \tag{1}$$

where λ_e and μ are Lamé elastic constants, $\dot{\sigma}^{p}_{ij}$ is the initial stress rate resulting from the non-linear stress–strain relationship for the plastic (or damage-plastic) strain, and $\dot{u}_i$ is the displacement rate. The Latin subscripts refer to Cartesian co-ordinates, the subscripts preceding by a comma denote the derivatives, and repetition of subscripts implies summation over $i=1,2,3$. The incremental initial (plastic) stress rate is proportional to the plastic strain rate $\dot{\varepsilon}_{ij}^{\mathrm{p}}$ as

$$\dot{\sigma}_{ij}^{\mathrm{p}} = c_{ijkl}\dot{\varepsilon}_{kl}^{\mathrm{p}} \tag{2}$$

where c_{ijkl} is tensor depending on the stress tensor and expressed according to the normality rule and continuity condition of plasticity, as described later. The stress rate tensor is proportional to the elastic part of strains

$$\dot{\sigma}_{ij} = c_{ijkl}(\dot{\varepsilon}_{kl} - \dot{\varepsilon}_{kl}^{\mathrm{p}}) = \dot{\sigma}_{ij}^{\mathrm{e}} - \dot{\sigma}_{ij}^{\mathrm{p}} \tag{3}$$

where $\dot{\sigma}_{ij}^{\mathrm{e}}$ is the elastic stress rate tensor.

The integral representation of the displacement rates satisfying the governing equation (1) can be written as [37]:

$$\dot{u}_j(y) = \int_{\Omega} \dot{\sigma}_{ik}^{\mathrm{p}}(x)U_{ikj}(x-y)\,\mathrm{d}\Omega + \int_{\Gamma} \dot{t}_i(\eta)U_{ij}(\eta-y)\,\mathrm{d}\Gamma - \int_{\Gamma} \dot{u}_i(\eta)T_{ij}(\eta,y)\,\mathrm{d}\Gamma \tag{4}$$

for $y\in\Omega$, where Ω is the analysed body, Γ is its boundary, $\dot{t}_i$ is the rate of the applied surface traction vector, and U_{ij} is the fundamental displacement corresponding to a body force in an infinite space, which must satisfy the governing equation

$$c_{ijkl}U_{km,jl}(x-y) = -\delta_{im}\delta(x-y) \tag{5}$$

where $\delta(s)$ is the Dirac delta function of argument s. The other kernel functions in Equation (4) are defined by

$$\begin{aligned} T_{ij}(\eta,y) &= c_{isml}n_s(\eta)U_{mj,l}(\eta-y) \\ U_{ikj}(x-y) &= U_{ij,k} \end{aligned} \tag{6}$$

Explicit expressions for all the kernel functions are presented in Appendix A.

In a well-posed boundary value problem, only one of the boundary quantities in Equation (4) is prescribed. The second one needs to be computed. To obtain a relation between the boundary displacement rates and traction rates, we may take the limit case of the integral representation (4) in which an internal point y approaches a boundary point $\zeta\in\Gamma$. Thus we obtain the boundary integral equation (BIE)

$$\int_{\Gamma} [\dot{u}_i(\eta) - \dot{u}_i(\zeta)]T_{ij}(\eta,\zeta)\,\mathrm{d}\Gamma - \int_{\Gamma} \dot{t}_i(\eta)U_{ij}(\eta-\zeta)\,\mathrm{d}\Gamma = \int_{\Omega_{\mathrm{p}}} \dot{\sigma}_{ik}^{\mathrm{p}}(x)U_{ikj}(x-\zeta)\,\mathrm{d}\Omega \tag{7}$$

where Ω_{p} is an open region ($\Omega_{\mathrm{p}}\subset\Omega$) involving the real plastic zone. Substituting the integral representation of displacement rate (4) into the constitutive equation (3) and applying regularization [38], one obtains the integral representation of the stress rate at internal points

$$\begin{aligned} \dot{\sigma}_{ij}(y) = {} & -\dot{\sigma}_{ij}^{\mathrm{p}}(y) + c_{ijms}\frac{\partial}{\partial y_s}\int_{\Omega_{\mathrm{p}}} \dot{\sigma}_{kl}^{\mathrm{p}}(x)U_{km,l}(x-y)\,\mathrm{d}\Omega \\ & + \int_{\Gamma} [\dot{t}_k(\eta)D_{ijk}(\eta-y) + T_{ijkl}(\eta-y)\hat{D}_l\dot{u}_k(\eta)]\,\mathrm{d}\Gamma \end{aligned} \tag{8}$$

where

$$\hat{D}_l = \delta_{l3} \frac{\partial}{\partial \tau}(\eta) \tag{9}$$

with $\tau(\eta)$ being the unit vector tangent to the boundary Γ at point η, for two-dimensional problems.

The differentiation of the domain integral cannot be performed directly behind the integral sign because of a strong singularity of the kernel. Splitting Ω_{p} into regular and singular parts, $\Omega_{\mathrm{p}} = \Omega_{\mathrm{pR}} + \Omega_{\mathrm{pS}}(y \notin \Omega_{\mathrm{pR}}, y \in \Omega_{\mathrm{pS}})$, we may write

$$\begin{aligned}\dot{\sigma}_{ij}(y) = -\dot{\sigma}^{\mathrm{p}}_{ij}(y) + \int_{\Omega_{\mathrm{p}}} \lfloor \dot{\sigma}^{\mathrm{p}}_{kl}(x) - \dot{\sigma}^{\mathrm{p}}_{kl}(y) \rfloor E_{ijkl}(x-y)\,\mathrm{d}\Omega + \int_{\Gamma} [\dot{t}_k(\eta) D_{ijk}(\eta - y) \\ + T_{ijkl}(\eta - y)\hat{D}_l \dot{u}_k(\eta)]\,\mathrm{d}\Gamma + \dot{\sigma}^{\mathrm{p}}_{kl}(y) \left[\int_{\Omega_{\mathrm{pR}}} D_{ijk,l}(x-y)\,\mathrm{d}\Omega + A_{ijkl} \right]\end{aligned} \tag{10}$$

with $E_{ijkl} = -c_{ijps} U_{kp,ls} = D_{ijk,l}$

$$A_{ijkl} = \text{v.p.} \int_{\Omega_{\mathrm{pS}}} D_{ijk,l}(x-y)\,\mathrm{d}\Omega$$

where v.p. denotes the Cauchy principal value.

Taking Ω_{pS} as a circular domain centered at y with arbitrary radius, one can evaluate A_{ijkl} analytically, with the result

$$A_{ijkl} = \frac{1}{8(1-v)} [(3-4v)(\delta_{ik}\delta_{jl} + \delta_{il}\delta_{jk}) - (1-4v)\delta_{ij}\delta_{kl}] \tag{11}$$

The integral representation (10) can be used safely for evaluating the stress tensor rates at interior nodes as long as the distance of the node from the boundary contour is comparable with the length of the boundary elements.

Nevertheless, we need to know $\dot{\sigma}^{\mathrm{p}}_{ij}$ even at the boundary nodes if Ω_{p} reaches the boundary contour. Then, we must calculate the stress tensor rates in the incremental iterative scheme, in which the integral representation needs to be replaced by a regularized integral equation. This can be done by using the constitutive law (3); hence

$$\dot{\sigma}_{ij}(\zeta) = c_{ijkl} \dot{u}_{k,l}(\zeta) - \dot{\sigma}^{\mathrm{p}}_{ij}(\zeta) \tag{12}$$

and the gradients of the displacement rates can be obtained by solving the regularized BIE derived elsewhere [27]. Alternatively, one can get another set of the regularized BIE from the integral representation (8) by using the integral identity

$$\dot{\sigma}_{ij}(y) + \dot{\sigma}^{\mathrm{p}}_{ij}(y) = (\dot{\sigma}_{kl}(y) + \dot{\sigma}^{\mathrm{p}}_{kl}(y)) \int_{\Gamma} n_l(\eta) D_{ijk}(\eta - y)\,\mathrm{d}\Gamma + \dot{u}_{k,l}(y) \int_{\Gamma} \tau_l(\eta) T_{ijk3}(\eta - y)\,\mathrm{d}\Gamma \tag{13}$$

This integral identity results by introducing into (8) the elastic solution $\dot{\tilde{u}}_{i,k}(x) = \text{const.} = \dot{u}_{i,k}(y)$,

$$\dot{\sigma}^{\mathrm{p}}_{ij}(x) = 0, \dot{\tilde{\sigma}}_{ij}(x) = c_{ijkl} \dot{\tilde{u}}_{k,l}(x) = c_{ijkl} \dot{u}_{k,l}(y) = \dot{\sigma}_{ij}(y) + \dot{\sigma}^{\mathrm{p}}_{ij}(y)$$

Making use of the subtraction and addition technique [39], and taking $y=\zeta\in\Gamma$, one can obtain the following relation for the regularized BIE

$$\begin{aligned}&\dot{u}_{k,l}(\zeta)\sum_p\int_{\Gamma_p}\lfloor\tau_l(\eta)-\hat{\chi}_p\tau_l(\zeta)\rfloor T_{ijk3}(\eta-\zeta)\,\mathrm{d}\Gamma+\dot{\sigma}_{kl}(\zeta)\sum_p\int_{\Gamma_p}\lfloor n_l(\eta)-\hat{\chi}_p n_l(\zeta)\rfloor D_{ijk}(\eta-\zeta)\,\mathrm{d}\Gamma\\&\quad=\int_\Omega\lfloor\dot{\sigma}^{\mathrm{p}}_{kl}(x)-\dot{\sigma}^{\mathrm{p}}_{kl}(\zeta)\rfloor E_{ijkl}(x-\zeta)\,\mathrm{d}\Omega+\sum_p\int_{\Gamma_p}[t_k(\eta)-\hat{\chi}_p t_k(\zeta)]D_{ijk}(\eta-\zeta)\,\mathrm{d}\Gamma\\&\qquad+\sum_p\int_{\Gamma_p}\left[\frac{\partial u_k}{\partial\tau}(\eta)-\hat{\chi}_p\frac{\partial u_k}{\partial\tau}(\zeta)\right]T_{ijk3}(\eta-\zeta)\,\mathrm{d}\Gamma\end{aligned}\tag{14}$$

in which $\dot{\sigma}_{ij}(\zeta)$ should be replaced by Equation (12). Note that Γ_p are the boundary elements ($\Gamma=\sum_p\Gamma_p$), and the selection operator is defined as [39]:

$$\hat{\chi}_p f(\zeta)=\begin{cases}\lim\limits_{\Gamma_p\in\eta\to\zeta} f(\eta), & \zeta\in\Gamma_p\\ 0, & \zeta\notin\Gamma_p\end{cases}\tag{15}$$

The regularized BIE (7) and (14) together with the regularized integral representation (10) are to be used in the incremental iterative solution algorithm. Using the quadratic approximation of the boundary quantities within the boundary elements as well as the plastic stress rate over the domain elements, one can perform the integrations involved in the BIE and the integral representation of the stress rate. The BIE (7) and (14) are written in such a form that all the boundary integrals exist in the ordinary sense. The integral representation of the internal stress rate (10) is also given in the non-singular form. Consequently, all the boundary and domain integrals can be computed sufficiently accurately by the regular Gaussian quadrature rule, even if the interior points coincide with the boundary.

3. NON-LOCAL PLASTICITY MODEL AND ITS IMPLEMENTATION

Aside from continuum damage mechanics, one way to describe the strain softening damage is to modify the classical hardening plasticity by allowing the hardening function to decrease. We choose to pursue this approach. First we must define the local plasticity model, which will further be generalized to a nonlocal form. The yield surfaces are written as $F(\sigma_{ij},k)=0$ and the yield function is assumed to have the form

$$F(\sigma_{ij},k)=f(\sigma_{ij})-\psi(k)=0\tag{16}$$

in which $f(\sigma_{ij})$ may be regarded as the effective stress σ_{e}; $\psi(k)$ is normally called the work-hardening function (although it will be used here to characterize softening), and k is a hardening-softening parameter defined by work,

$$k=\int\sigma_{ij}\mathrm{d}\varepsilon_{ij}$$

As usual, we require the plastic strain increment $d\varepsilon_{ij}^{p}$ to follow the normality rule

$$d\varepsilon_{ij}^{p} = d\lambda a_{ij} \tag{17}$$

where $d\lambda$ represents a scalar proportionality coefficient and $a_{ij} = \partial F/\partial\sigma_{ij}$. Differentiating the yield function (16), one can obtain the expression for the proportionality coefficient

$$d\lambda = \frac{a_{ij}c_{ijkl}\,d\varepsilon_{kl}}{a_{ij}a_{kl}c_{ijkl} + (d\psi/dk)\sigma_{ij}a_{ij}} \tag{18}$$

Although the strain-softening is a typical property of frictional dilatant materials, we choose to consider in the numerical example a softening version of von Mises plasticity because it is simpler and more transparent, and sufficient to demonstrate the workability of the idea of non-local BEM. The stress intensity $\sigma_e = (\frac{3}{2}s_{ij}s_{ij})^{1/2}$, in which $s_{ij} = \sigma_{ij} - \frac{1}{3}\delta_{ij}\sigma_{kk}$ is the deviator of stresses, receives the yield stress value $\sigma_0(k)$ on the yield surface, i.e. $\sigma_e - \sigma_0(k) = 0$. One can easily derive the following well-known relations

$$\begin{aligned} d\varepsilon_{ij}^{p} &= \frac{3}{2}\frac{s_{ij}}{\sigma_e}\,d\lambda \\ d\lambda &= 3\mu\frac{s_{kl}}{3\mu + H}\frac{d\varepsilon_{kl}}{\sigma_e} \end{aligned} \tag{19}$$

where $H = d\psi/d\varepsilon^{p}$ and $\varepsilon^{p} = (\frac{2}{3}\varepsilon_{ij}^{p}\varepsilon_{ij}^{p})^{1/2}$ is the plastic strain intensity.

The essential idea of the non-local continuum is that some of the variables in the constitutive equation are defined by spatial averaging. Only those variables that cause strain softening may be considered as non-local [3]. Computationally, it is more efficient to apply the spatial averaging to the proportionality coefficient $d\lambda$ than to plastic strains. Then, the non-local proportionality coefficient $d\bar{\lambda}$ (or scaling parameter) is defined as

$$d\bar{\lambda}(y) = \frac{1}{V_\alpha(y)}\int_\Omega \alpha(x,y)\,d\lambda(x)\,d\Omega(x) \tag{20}$$

where

$$V_\alpha(y) = \int_\Omega \alpha(x,y)\,d\Omega(x)$$

and $\alpha(x,y)$ is the chosen weight function. To define the non-local weight function $\alpha(x,y)$, the normal distribution function may be used [3]:

$$\alpha(x,y) = \exp(-(2r/l)^2) \tag{21}$$

where l is the material characteristic length which measures the heterogeneity scale of the material, and $r = |x - y|$.

After calculating the spatial non-local average $d\bar{\lambda}$, one may compute the non-local values of other variables such as the plastic strain increment $d\bar{\varepsilon}_{ij}^{p}$ and the plastic stress increment $d\bar{\sigma}_{ij}^{p}$;

$$\begin{aligned} d\bar{\varepsilon}_{ij}^{p} &= d\bar{\lambda}a_{ij} \\ d\bar{\sigma}_{ij}^{p} &= d\bar{\lambda}a_{kl}c_{ijkl} \end{aligned}$$

Since $\mathrm{d}\bar{\sigma}_{ij}^{\mathrm{p}}$ is not known at the beginning of each load increment, an iterative procedure is needed. Making use of the discretization in the BEM formulation, the BIE (7) can be translated into the matrix form as

$$\mathbf{T}\dot{\mathbf{u}} = \mathbf{U}\dot{\mathbf{t}} + \mathbf{Q}\dot{\boldsymbol{\sigma}}^{\mathrm{p}} \tag{22}$$

The stress tensor rates at nodal points can be expressed in terms of the nodal values of the displacement and traction rates as well as the plastic part of the stress tensor rates

$$\dot{\boldsymbol{\sigma}} = \mathbf{D}\dot{\mathbf{t}} + \mathbf{T}'\dot{\mathbf{u}} + \mathbf{E}\dot{\boldsymbol{\sigma}}^{\mathrm{p}} \tag{23}$$

Denoting the boundary unknowns by $\dot{\mathbf{X}}$, we rewrite Equations (22) and (23) as

$$\begin{aligned} \mathbf{A}\dot{\mathbf{X}} &= \dot{\mathbf{F}} + \mathbf{Q}\dot{\boldsymbol{\sigma}}^{\mathrm{p}} \\ \dot{\boldsymbol{\sigma}} &= \mathbf{A}'\dot{\mathbf{X}} + \dot{\mathbf{F}}' + \mathbf{E}\dot{\boldsymbol{\sigma}}^{\mathrm{p}} \end{aligned} \tag{24}$$

The prescribed values at boundary nodes enter the vectors $\dot{\mathbf{F}}$ and $\dot{\mathbf{F}}'$. Then, the boundary unknowns are given by

$$\dot{\mathbf{X}} = \mathbf{R}\dot{\boldsymbol{\sigma}}^{\mathrm{p}} + \dot{\mathbf{M}} \tag{25}$$

where

$$\mathbf{R} = \mathbf{A}^{-1}\mathbf{Q}, \quad \dot{\mathbf{M}} = \mathbf{A}^{-1}\dot{\mathbf{F}}$$

Adding the plastic stress rate $\dot{\boldsymbol{\sigma}}^{\mathrm{p}}$ to both sides of the second equation (24) and using Equation (25), we get

$$\dot{\boldsymbol{\sigma}}^{\mathrm{e}} = \mathbf{S}\dot{\boldsymbol{\sigma}}^{\mathrm{p}} + \dot{\mathbf{N}} \tag{26}$$

where

$$\begin{aligned} \mathbf{S} &= \mathbf{E} + \mathbf{I} + \mathbf{A}'\mathbf{R} \\ \dot{\mathbf{N}} &= \dot{\mathbf{F}}' + \mathbf{A}'\dot{\mathbf{M}} \end{aligned}$$

with $\mathbf{I}$ being the identity matrix.

The iteration process may be summarized as follows:

(1) Compute the elastic stress increment $\mathrm{d}\sigma_{ij}^{\mathrm{e}}$ from Equation (26).
(2) For the points whose stress state is beyond the yield surface, compute the proportionality coefficient $\mathrm{d}\lambda = \dfrac{a_{ij}\mathrm{d}\sigma_{ij}^{\mathrm{e}}}{a_{ij}a_{kl}c_{ijkl} + (\mathrm{d}\psi/\mathrm{d}k)\sigma_{ij}a_{ij}}$.
(3) Compute the non-local value $\mathrm{d}\bar{\lambda}$ from Equation (20).
(4) Compute the averaging plastic stress increment $\mathrm{d}\bar{\sigma}_{ij}^{\mathrm{p}} = \mathrm{d}\bar{\lambda}c_{ijkl}a_{kl}$.
(5) Verify the convergence of iteration, i.e. compare $\mathrm{d}\sigma_{ij}^{\mathrm{p}}$ to the value used in Equation (26) in step 1.

(6) If the relative difference of two subsequent iteration steps is less than the selected tolerance, go to step 1 and begin a new load increment.

4. NUMERICAL EXAMPLE

A rectangular plate with a central hole under a uniform tension applied at the end of plate is analysed. Restricting consideration to symmetric deformation, we need to analyse numerically only a quarter of the specimen. The diameter of the circular hole, $d = 0.1$ m, is one half of the specimen width. The material constants used in the von Mises constitutive model are the following: Young's modulus $E = 7 \times 10^4$ MPa, Poisson ratio $\nu = 0.3$, and yield stress $\sigma_0 = 243$ MPa. Plane stress conditions are considered.

Two different meshes are used in the numerical analysis. For the coarse mesh, the boundary is discretized by 13 quadratic boundary elements and the domain by 11 quadrilateral or triangular elements with quadratic approximations. For the fine mesh, 16 quadratic boundary elements and 18 domain elements are used. Figure 1(a) and (b) show the boundary and domain discretizations for both meshes. Material characteristic length for the non-local model is taken as $l = 2$ cm. For the coarse mesh, the load increments are chosen such that the collapse load would be reached within 72 and 80 increments for the local and non-local models, respectively. For the fine mesh, smaller load increments are selected, leading to collapse within 108 and 121 increments, respectively. Two different softening parameters are used in analysis; $H = -3 \times 10^3$ MPa and $H = -10^3$ MPa.

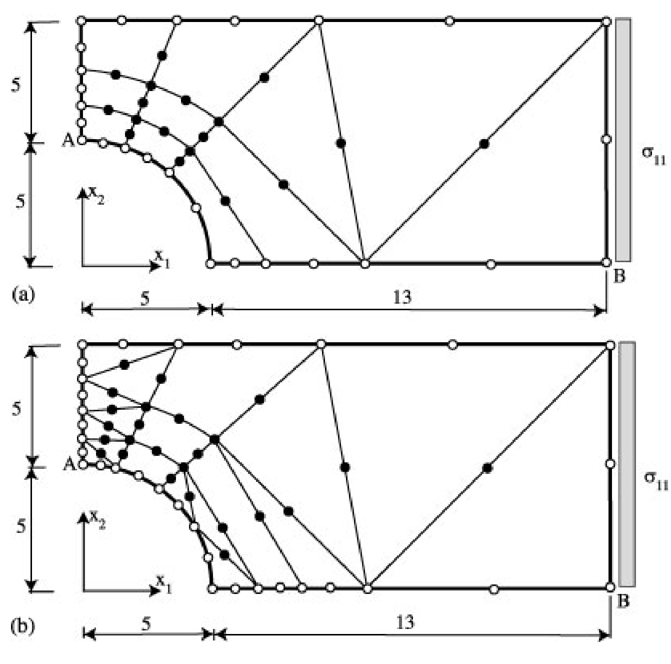

Figure 1. Discretization mesh for perforated plate (dimensions in cm): (a) coarse mesh; and (b) fine mesh.

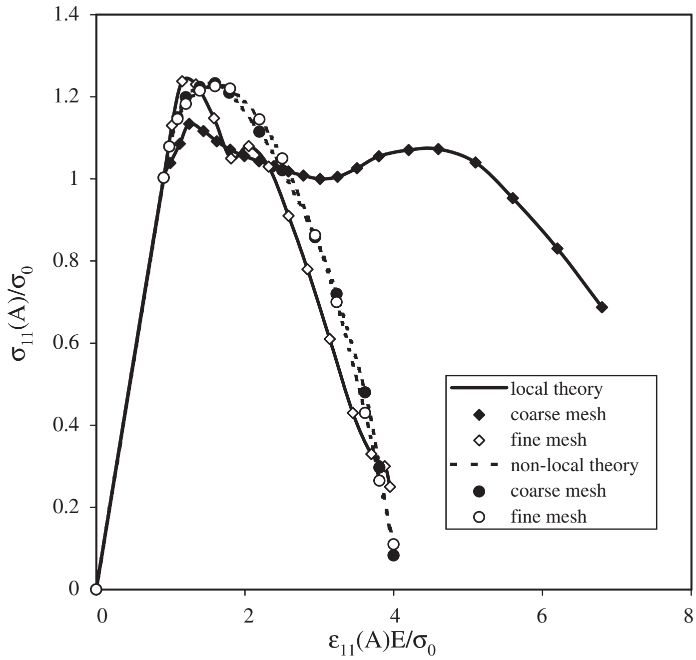

Figure 2. Stress–strain relationship in local and non-local plastic models with softening modulus $H=-3\times 10^3$ MPa (black squares—coarse mesh, solid squares—fine mesh, solid curve—local theory, dashed curve—nonlocal theory).

Comparisons between the local and non-local boundary element analyses of the two meshes are shown in Figure 2. The figure presents the dependence of the stress component σ_{11} on the strain component ε_{11} at node A lying on the surface of the hole at $x_1=0$ (the place of maximum stress). One can observe in the figure nearly identical responses for both meshes in the non-local plastic model with softening parameter $H=-3\times 10^3$ MPa (dashed line). (Note that the black symbols correspond to the coarse mesh and the white ones to the fine mesh.)

The solid curve represents the results obtained for the local plastic model. The local boundary element results are seen to be unstable, giving spurious oscillations for both meshes. Therefore, they are not objective.

Since the hole tends to elevate the stresses, one might wonder whether a much more refined mesh might be needed to obtain accurate stress values. For the non-local model, however, the stress concentrations are known to be limited by the material characteristic length. The non-locality prevents sharp stress concentrations, and this renders the use of very fine meshes superfluous.

Although the stress applied at the boundary is not completely uniform (due to a finite length of the specimen), the loading may be characterized by the stress applied at one point of the boundary. We choose point B in Figure 1. The strain at the root of the perforated plate (node A) as a function of the applied stress at node B is given in Figure 3. The higher values of the applied stress correspond to the non-local model, which is explained by the fact that the non-locality tends to suppress material softening near the hole.

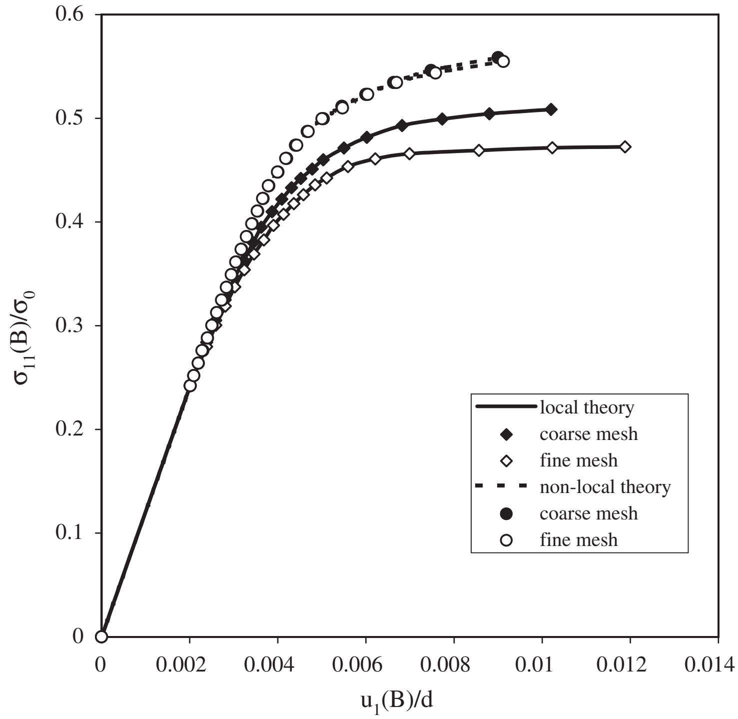

Figure 3. Stress-displacement response at the end of the perforated plate.

Figure 4 presents the stress–strain history at node A for two different softening parameters $H = -3 \times 10^3$ MPa and $H = -10^3$ MPa in the non-local model. As it could be expected, higher values of stresses are observed for smaller values of the softening parameter. Similar variations can be observed in both curves. One can observe that the numerical results are independent of the mesh discretizations, for both softening parameters, if the non-local model is used.

5. CONCLUSIONS

1. The boundary element method is generalized to handle strain-softening damage through a strongly non-local integral-type non-local operator. A plasticity model with yield limit degradation is implemented in a boundary element program to study the strain-softening damage in localization problems. The initial stress boundary element method employing an iteration procedure in each load increment is applied to deal with the softening damage. Regularized integral representations and boundary integral equations are used to avoid the difficulties associated with numerical computation of singular integrals.
2. Similar to finite element analyses, the results for strain-softening damage computed from the conventional boundary element formulation exhibit spurious sensitivity to cell mesh refinements even though the nature of cells is entirely different from that of finite elements. The damage appears to localize into a zone of a single cell width, and the energy dissipation strongly depends on the cell meshes.

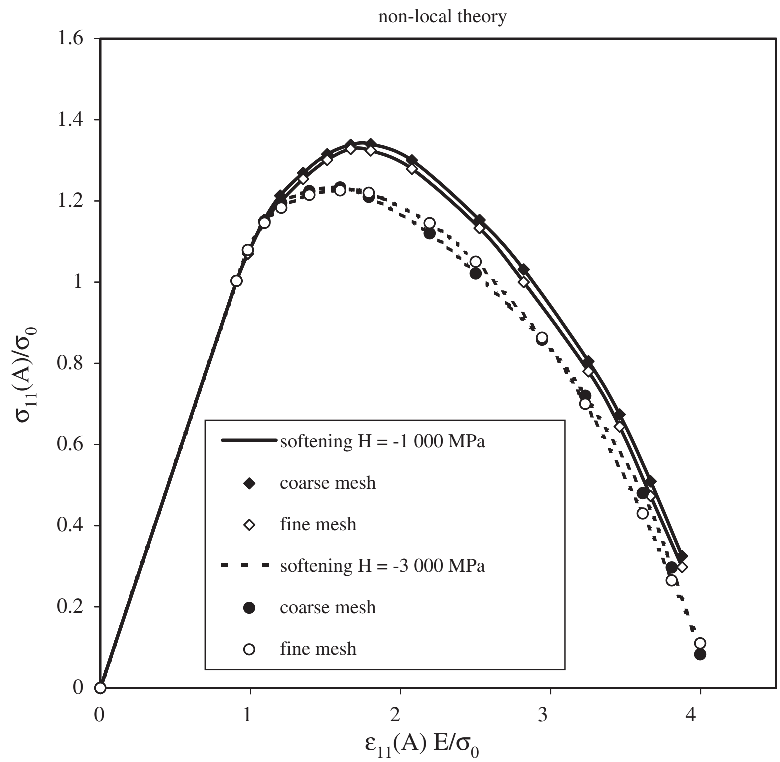

Figure 4. Stress–strain relationship at the root of perforated plate for non-local model with two different softening parameters.

3. A strongly non-local formulation of integral type is incorporated into the boundary element program to remedy the problem of spurious damage localization. The numerical example confirms the effectiveness of the non-local formulation in preventing the spurious cell mesh sensitivity observed in the local formulation.
4. One advantage of adopting the boundary element method for analysing the damage localization problems is that the strain softening damage tends to localize into a narrow band and thus the internal cells are needed only in a small region rather than the entire domain of the body under consideration.

APPENDIX A

The explicit expressions for the two-dimensional fundamental solutions and the integral kernels involved in integral representations given in Section 2 are as follows:

$$U_{ik}(x-y) = \frac{1}{8\pi\mu(1-v)}[-(3-4v)\delta_{ik}\ \ln r + r_{,i}r_{,k}]$$

$$T_{ik}(x,y) = \frac{1-2v}{4\pi(1-v)r}\left[r_k n_i(x) - r_{,i} n_k(x) - \left(\delta_{ik} + \frac{2}{1-2v} r_{,i} r_{,k}\right) r_{,j} n_j(x)\right]$$

$$U_{ijk}(x-y) = \frac{1-2v}{4\pi\mu(1-v)r}[(1-2v)(r_{,j}\delta_{ik} + r_{,i}\delta_{jk}) - r_{,k}\delta_{ij} + 2r_{,i}r_{,j}r_{,k}]$$

$$D_{lji}(x-y) = \frac{1}{4\pi(1-v)r}[(1-2v)(r_{,j}\delta_{li} + r_{,l}\delta_{ji} - r_{,i}\delta_{lj}) + 2r_{,i}r_{,j}r_{,l}]$$

$$T_{ljim}(x-y) = \frac{\mu}{4\pi(1-v)r}\{4v\delta_{lj}\varepsilon_{kim}r_{,k} + (1-2v)[r_{,l}\varepsilon_{jim} + r_{,j}\varepsilon_{\text{lim}} - r_{,k}(\delta_{il}\varepsilon_{jkm} + \delta_{ij}\varepsilon_{lkm})]$$
$$- 2r_{,i}r_{,k}(r_{,l}\varepsilon_{jkm} + r_{,j}\varepsilon_{lkm})\}$$

$$E_{ijkl}(x-y) = \frac{1}{4\pi(1-v)r^2}\{(1-2v)(\delta_{il}\delta_{jk} + \delta_{ik}\delta_{jl} - \delta_{ij}\delta_{kl} + 2\delta_{ij}r_{,k}r_{,l}) + 2\delta_{kl}r_{,i}r_{,j}$$
$$+ 2v(\delta_{ik}r_{,j}r_{,l} + \delta_{il}r_{,j}r_{,k} + \delta_{jk}r_{,i}r_{,l} + \delta_{jl}r_{,i}r_{,k}) - 8r_{,i}r_{,j}r_{,k}r_{,l}\}$$

where

$$r_i = x_i - y_i, \quad r = (r_i r_i)^{1/2}, \quad r_{,i} = \frac{r_i}{r}$$

In the case of plane stress problem, v should be replaced by $v/(1+v)$.

ACKNOWLEDGEMENT

Partial financial support for this research as well as for the Senior Visiting Scholar appointment of the first author at Northwestern University was obtained under U.S. National Science Grant CMS-9713944 to Northwestern University.

REFERENCES

1. Bažant ZP. Instability, ductility and size effect in strain softening concrete. *Journal of the Engineering Mechanics Division* (ASCE) 1976; **12**:331–344.
2. Sandler IS. Strain-softening for static and dynamic problems. In *Proceedings of the Symposium on Constitutive Equations*; *Micro*, *Macro and Computational Aspects*, Willam KJ (ed.). ASME: New York, 1984; 217–231.
3. Bažant ZP, Lin F-B. Non-local yield degradation. *International Journal for Numerical Methods in Engineering* 1988; **26**:1805–1823.
4. Bažant ZP, Belytschko TB, Chang TP. Continuum theory for strain-softening. *Journal of the Engineering Mechanics Division* (ASCE) 1984; **110**:1666–1692.
5. Bažant ZP. Crack band model for fracture of geomaterials. In *Proceedings of the 4th International Conference on Numerical Methods in Geomechanics*, Eisenstein Z (ed.). Edmonton, 1982; 1137–1152.
6. Bažant ZP, Ožbolt J. Nonlocal microplane model for fracture, damage and size effect in structures. *Journal of Engineering Mechanics* (ASCE) 1990; **116**:2485–2505.
7. Bažant ZP, Ožbolt J. Compression failure of quasibrittle material; Nonlocal microplane model. *Journal of Engineering Mechanics* (ASCE) 1992; **118**:540–556.
8. Bažant ZP, Cedolin L. *Stability of Structures*. Oxford University Press: Oxford, 1991.
9. Bažant ZP, Planas J. *Fracture and Size Effect in Concrete and Other Quasibrittle Materials*. CRC Press: Boca Raton, 1998.
10. Kröner E. Elasticity theory of materials with long-range cohesive forces. *International Journal of Solids and Structures* 1967; **4**:731–742.
11. Eringen AC, Edelen DGB. On nonlocal elasticity. *International Journal of Engineering Science* 1972; **10**: 233–248.

12. Bažant ZP, Pijaudier-Cabot G. Modeling of distributed damage by nonlocal continuum with local strain. In *Proceedings of the 4th International Conference on Numerical Methods in Fracture Mechanics*, Luxmore AR. *et al*. (eds). San Antonio, 1987; 411–432.
13. Pijaudier-Cabot G, Bažant ZP. Nonlocal damage theory. *Journal of Engineering Mechanics* (ASCE) 1987; **113**:1512–1533.
14. Jirásek M. Nonlocal models for damage and fracture: comparison of approaches. *International Journal of Solids and Structures* 1998; **35**:4133–4145.
15. Bažant ZP, Jirásek M. Nonlocal integral formulations of plasticity and damage: Survey of progress. *Journal of Engineering Mechanics* (ASCE) 2002; **128**:1119–1149.
16. Swedlow JL, Cruse TA. Formulation of boundary integral equations for three-dimensional flow. *International Journal of Solids and Structures* 1971; **7**:1673–1683.
17. Ricardella PC. An implementation of the boundary integral technique for planar problems of elasticity and elasto-plasticity. *Ph.D. Thesis*, Carnegie-Mellon University, Pittsburgh, 1973.
18. Chaudonneret M. Boundary integral equation method for visco-plasticity analysis. *Journal de mécanique appliquée* 1977; **1**:113–131.
19. Kumar V, Mukherjee S. A boundary integral equation formulation for time dependent inelastic deformation in metals. *International Journal of Mechanical Sciences* 1975; **19**:713–724.
20. Banerjee PK, Cathie DN, Davies TG. Two and three-dimensional problems of elastoplasticity. In *Developments in Boundary Element Methods*, vol 1. Applied Science Publishers: London, 1979; 63–95.
21. Banerjee PK, Cathie DN. Boundary element methods for axisymmetric plasticity. In *Innovative Numerical Methods for the Applied Engineering Science*, Shaw RP. *et al*. (eds). University of Virginia Press: Charlottesville, 1980.
22. Telles JCF, Brebbia CA. Boundary elements in plasticity. *Applied Mathematical Modelling* 1981; **5**:275–281.
23. Henry DP, Banerjee PK. A new BEM formulation for two and three-dimensional elastoplasticity using particular integrals. *International Journal for Numerical Methods in Engineering* 1988; **26**:2079–2096.
24. Leitao V, Alabadi MH, Rooke DP. The dual boundary element formulation for elastoplastic fracture mechanics. *International Journal for Numerical Methods in Engineering* 1995; **38**:315–333.
25. Herding U, Kuhn G. A field boundary element formulation for damage mechanics. *Engineering Analysis with Boundary Elements* 1996; **18**:137–147.
26. Sládek V, Sládek J, Tanaka M. Regularization of hypersingular and nearly singular integrals in the potential theory and elasticity. *International Journal for Numerical Methods in Engineering* 1993; **36**:1609–1628.
27. Sládek V, Sládek J. Displacement gradients in BEM formulation for small strain plasticity. *Engineering Analysis with Boundary Elements* 1999; **23**:471–477.
28. Kuhn G, Partheymuller P, Kohler O. Regularization and evaluation of singular domain integrals in boundary element methods. In *Singular Integrals in Boundary Element Methods*, Sladek V, Sladek J (eds). CMP: Southampton, 1998; 221–261.
29. Sládek J, Sládek V. Boundary element analysis for an interface crack between dissimilar elastoplastic materials. *Computational Mechanics* 1995; **65**:396–405.
30. Maier G, Polizzotto C. A Galerkin approach to boundary element elastoplastic analysis. *Computer Methods in Applied Mechanics and Engineering* 1987; **60**:175–194.
31. Comi C, Maier G. Extremum, convergence and stability properties of the finite-increment problem in elastic-plastic boundary element analysis. *International Journal of Solids and Structures* 1992; **29**(2):240–270.
32. Maier G, Novati G, Cen ZZ. Symmetric boundary element method for quasibrittle fracture and frictional contact problems. *Computational Mechanics* 1993; **13**:74–89.
33. Bonnet M, Maier G, Polizzotto C. Symmetric Galerkin boundary element method. *Applied Mechanics Reviews* (ASME) 1998; **51**(11):669–704.
34. Maier G, Miccoli S, Novati G, Perego U. Symmetric Galerkin boundary element method in plasticity and gradient plasticity. *Computational Mechanics* 1995; **17**:115–129.
35. Cen Z, Maier G, Novati G. On boundary element analysis in the presence of softening. In *Boundary Element Methods in Engineering*, Annigeri BS, Tseng K (eds). Springer: Berlin, 1989; 300–309.
36. Lin F-B, Yan GY, Bažant ZP, Ding F. Nonlocal strain-softening model of quasi-brittle materials using boundary element method. *Engineering Analysis with Boundary Elements* 2002; **26**:417–424.
37. Balaš J, Sládek J, Sládek V. *Stress Analysis by Boundary Element Methods*. Elsevier: Amsterdam, 1989.
38. Sládek V, Sládek J. Non-singular boundary integral representation of stresses. *International Journal for Numerical Methods in Engineering* 1992; **33**:1481–1499.
39. Tanaka M, Sládek V, Sládek J. Regularization techniques applied to boundary element methods. *Applied Mechanics Reviews* (ASME) 1994; **47**:457–499.

